Accepted Manuscript

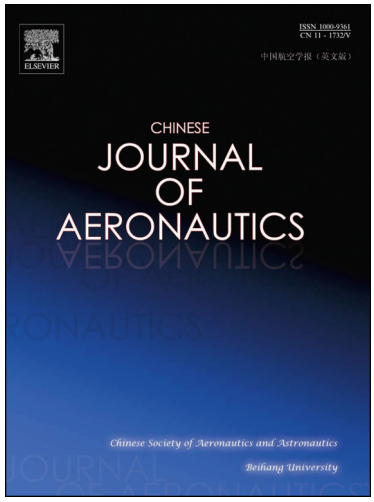

A guidance law for UAV autonomous aerial refueling based on the iterative computation method

Luo Delin, Xie Rongzeng, Duan Haibin

PII: S1000-9361(14)00033-8
DOI: http://dx.doi.org/10.1016/j.cja.2014.03.001
Reference: CJA 243

To appear in:

Received Date: 28 July 2013
Revised Date: 9 September 2013
Accepted Date: 16 November 2013

Please cite this article as: L. Delin, X. Rongzeng, D. Haibin, A guidance law for UAV autonomous aerial refueling based on the iterative computation method, (2014), doi: http://dx.doi.org/10.1016/j.cja.2014.03.001

A guidance law for UAV autonomous aerial refueling based on the iterative computation method

Luo Delin[1,*], Xie Rongzeng[1], Duan Haibin[2]

1. Department of Automation, Xiamen University, Xiamen 361005, China

2. State Key Laboratory of Virtual Reality of Technology and Systems, Beihang University, Beijing, 100191, PR China

Received on 28 July 2013; revised on 9 September 2013 ; accepted 16 November 2013

Abstract

The rendezvous and formation problem is a significant part for the unmanned aerial vehicle (UAV) autonomous aerial refueling (AAR) technique. It can be divided into two major phases: the long-range guidance phase and the formation phase. In this paper, an iterative computation guidance law (ICGL) is proposed to compute a series of state variables to get the solution of a control variable for a UAV conducting rendezvous with a tanker in AAR. The proposed method can make the control variable converge to zero when the tanker and the UAV receiver come to a formation flight eventually. For the long-range guidance phase, the ICGL divides it into two sub-phases: the correction sub-phase and the guidance sub-phase. The two sub-phases share the same iterative process. As for the formation phase, a velocity coordinates system and a nonlinear decreasing function which represents control acceleration are designed to make the speed of the UAV consistent with that of the tanker. The simulation results demonstrate that the proposed ICGL is effective and robust against wind disturbance.

Keywords: Autonomous aerial refueling; Aerial rendezvous; Formation control; Guidance law; Unmanned aerial vehicle

1. Introduction[1]

With the rapid development of UAV technologies, UAVs are being used to carry out various missions like high altitude surveillance and reconnaissance, long distance military strikes, etc., some of which require UAVs continuously stay in the air for a quite long time. To this end, autonomous aerial refueling (AAR) becomes a key issue to be addressed for these applications of UAVs. There are four main tasks to be accomplished sequentially during AAR of UAVs: UAVs rendezvous, formation maintaining, pipeline docking, and refueling. This paper mainly focuses on presenting a guidance law for the rendezvous and formation maintaining processes. For decades, a lot of achievements have been made to develop guidance technologies for the UAV rendezvous problem [1]. One of the most mature technologies is the classical proportional navigation guidance (PNG) [2]. After that, many improved proportional navigation guidance (IPNG) schemes have been evolved based on PNG [3, 4, 5]. To further enhance the guidance performance, modern control theories, such as sliding-mode control [6], differential geometric method [7], neural network [8], and so on, are also employed for the design of UAV rendezvous guidance laws. For formation maintaining, there are several existing methods such as feedback control presented in Ref. [9], in which a full-state linearization via a dynamic feedback controller is designed for controlling two robots in a leader-follower configuration. In Ref. [10], a synchronized position tracking controller is incorporated in formation flight control for multiple flying wings. Ref. [11] proposed a new approach of hybrid supervisory control for the leader-follower formation problem. The hybrid supervisory control approach provides a tractable framework for hybrid synthesis of formation control. Within this framework, a new method of abstraction based on polar partitioning of the state space is introduced. Ref. [12] presented an iterative guidance method for launch vehicles. In this method, the guidance for a launch vehicle is formulated as an optimal control problem, in which the transient state of the vehicle is taken as the initial value and the target point as the terminal constraint. The objective function is to minimize the flight time of the vehicle moving from the current position to the target point. During the whole flight process of the vehicle, for each time interval, the control solution and the corresponding flying trajectory are obtained by solving the established guidance equations. Through a repeated iterative computation, the launch vehicle is eventually guided to the target point and satisfies its predefined state. This method has been studied for the guidance and control design of launch vehicles and ballistic missiles [13, 14, 15, 16]. However, these approaches involve heavy computation load and are difficult for practical engineering

*Corresponding author. Tel.: +86-592-2580057.
E-mail address:luodelin1204@xmu.edu.cn

applications.

In this paper, a novel iterative computation guidance law (ICGL) is proposed for a UAV to perform rendezvous and formation maintaining with a tanker in the AAR process. In the ICGL, the rendezvous process of a UAV with a tanker in AAR is divided into two major phases: the long-range guidance phase and the formation phase. In each phase, the ICGL computes the relative state parameters between the UAV and the tanker in real-time to obtain the specific control variable. Furthermore, the ICGL divides the long-range guidance phase into two sub-phases which share the same iterative process: the correction sub-phase and the guidance sub-phase. In order to correct the actual distance error between the UAV and the tanker, an estimated distance term with a coefficient is added to the model in the formation phase. By adjusting the coefficient, the error can be eliminated. The ICGL proposed in this paper is totally different from the above mentioned iterative guidance method based on the optimal control theory. In the ICGL, a UAV approaches to a tanker along a smooth arc trajectory designed by a geometric method. Thus the iteration is based on the relative position between the UAV and the tanker in each time interval. The designed arc trajectory strategy has an advantage which makes the control vector perpendicular to the velocity of the UAV. Therefore, it is easy to be realized in practical engineering perspective.

The remainder of the paper is organized as follows. In Section 2, the problem of rendezvous for AAR is formulated mathematically. In Section 3, the ICGL algorithm is developed for a UAV to perform rendezvous and formation maintaining with a tanker in AAR. In Section 4, simulations are performed to verify the effectiveness of the proposed ICGL by comparing it with the nonlinear guidance (NG) method. Then simulation of wind disturbance injection is conducted to demonstrate the robustness of the ICGL. The conclusion remarks are given in Section 5.

2. Problem description

An illustrative diagram for the rendezvous process of a UAV with a tanker for aerial refueling is given in Fig.1. The research objective of this paper is to guide the UAV near the tanker and then the UAV keeps a formation flight with the tanker.

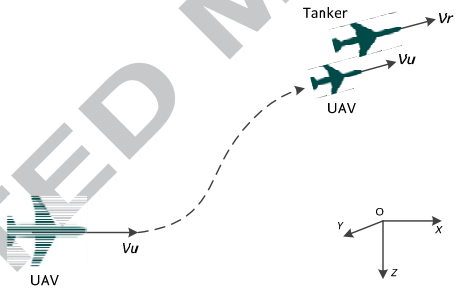

Fig.1 An illustrative rendezvous process of a UAV with a tanker

The system can be described in the Earth-fixed inertial frame *Oc-RF* shown in Fig.2 with its origin at the initial location of *U,* which stands for the UAV. The orientation of the X-axis is consistent with the initial velocity of the UAV. The Z-axis is downward and perpendicular to the X-axis in the vertical plane. The Y-axis is determined according to the right-hand rule. The transitional state of *U* during the rendezvous process is shown in Fig.3.

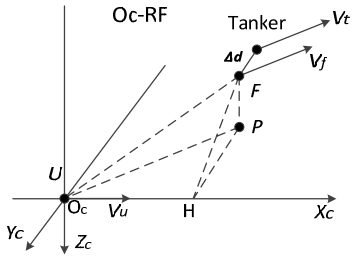

Fig.2 The unparallel situation

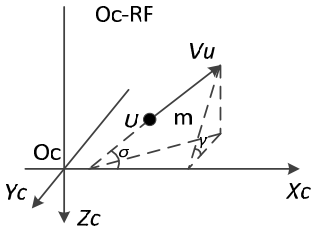

Fig.3 The state of the UAV during the guidance process

The position vector of *U* is denoted as

$$\boldsymbol{p}_U = (x_U, y_U, z_U)$$

The velocity vector of *U* is

$$v_u = (v_{u_x}, v_{u_y}, v_{u_z})$$

The motion of *U* can be described by the following kinematics equations [16]

$$\begin{aligned} \dot{x}_u &= v_u \cdot \cos\sigma \cdot \cos\gamma \\ \dot{y}_u &= v_u \cdot \sin\sigma \cdot \cos\gamma \\ \dot{z}_u &= v_u \cdot \sin\gamma \end{aligned} \quad (1)$$

where

$$v_u = \sqrt{v_{u_x}^2 + v_{u_y}^2 + v_{u_z}^2} \quad (2)$$

σ is the angle between the velocity of *U* and the X-axis. γ is the angle between the guidance surface m, which is determined by the guidance acceleration and the velocity of *U*, and the plane $O_t X_t Y_t$ as shown in Fig.3.

In Fig.2, *F* is the tracking point for *U* to keep a formation flight with the tanker. The location of *F* can be set according to the current position of the tanker with a deviation value Δd as shown in Fig.2. The position vector of *F* can be expressed as

$$p_f = p_t - \Delta d = (x_f, y_f, z_f)$$

The velocity vector of *F* is

$$v_f = v_t = (v_{f_x}, v_{f_y}, v_{f_z})$$

where p_t is the position vector of the tanker and v_t is the velocity vector for the tanker.

The motion of *F* can be described by the following kinematics

$$\begin{aligned} \dot{x}_f &= v_{f_x} \\ \dot{y}_f &= v_{f_y} \\ \dot{z}_f &= v_{f_z} \end{aligned} \quad (3)$$

3. Guidance law design

With the conditions discussed above, there exist two situations for the relationship of the initial velocity between *U* and *F*: unparallel as shown in Fig.2 and parallel as shown in Fig.4.

Since the parallel situation is an exceptional case of unparallel, the unparallel situation is mainly discussed in this paper. The rendezvous process can be divided into two phases: the long-range guidance phase and the formation phase.

3.1 Long-range guidance phase

The long-range guidance phase is defined from the initial instant to the instant when the distance between *U* and *F* is equal to or smaller than a given value. When v_u and v_f are not parallel, the long-range guidance phase should also be further divided into two sub-phases: the correction sub-phase and the guidance sub-phase.

3.1.1 Correction sub-phase

The correction sub-phase is to adjust the direction of v_u to parallel with the velocity of the projective point *P* within the $O_t X_t Y_t$ plane firstly. The geometric relationship between *U* and *P* in the $O_t X_t Y_t$ plane is shown in Fig.5.

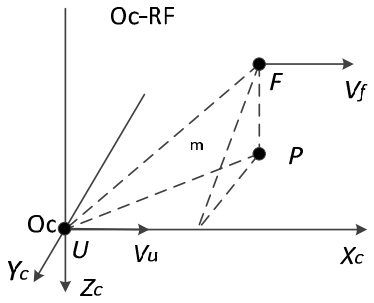

Fig.4 The parallel situation

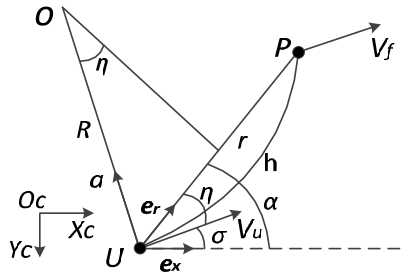

Fig.5 The geometric relationship in the two-dimensional plane

In Fig.5, r is the distance between U and P; α is the angle of line-of-sight; η is the advance angle of U; a is the lateral acceleration; $\boldsymbol{e}_x$ is the unit vector of the X-axis and $\boldsymbol{e}_r$ is the unit vector of the relative distance vector. The strategy used in this paper to guide U from the initial position to the location of P is an arc orbital approximation. U can move along the arc trajectory h from its current position to the target location by applying a normal corrective overload on U.

The guidance angle of U satisfies the constraint

$$\dot{\phi} = \frac{v_u}{R}$$

where the radius of h can be calculated by

$$R = \frac{r}{2 \cdot \sin \eta}$$

where $\eta = \alpha - \sigma$, in which $\alpha = \arccos\left(\frac{\boldsymbol{e}_x \cdot \boldsymbol{e}_r}{|\boldsymbol{e}_x| \cdot |\boldsymbol{e}_r|}\right)$.

According to the analysis above, the control acceleration can be calculated by

$$n = \frac{v_u^2}{R} \tag{4}$$

The iterative process throughout the correction sub-phase is shown below in detail.

(1) Initialization

Initialize the following parameters at the initial instant t_0:

The position vector of U

$$\boldsymbol{p}_u(t_0) = (x_{u_0}, y_{u_0}, z_{u_0}) = (0,0,0)$$

The velocity vector of U

$$\boldsymbol{v}_u(t_0) = (v_{ux_0}, v_{uy_0}, v_{uz_0}) = (v_{u_0}, 0, 0)$$

The position vector of P

$$\boldsymbol{p}_p(t_0) = (x_{p_0}, y_{p_0}, z_{p_0}) = (x_{p_0}, y_{p_0}, 0)$$

The velocity vector of P

$$\boldsymbol{v}_p(t_0) = (v_{px_0}, v_{py_0}, v_{pz_0}) = (v_{px}, v_{py}, v_{pz})$$

The guidance angle of U

$$\sigma(t_0) = 0$$

The relative distance vector between U and P

$$\boldsymbol{r}_{los}(t_0) = \boldsymbol{p}_p(t_0) - \boldsymbol{p}_u(t_0)$$

The magnitude of the distance between U and P

$$r(t_0) = \|\boldsymbol{r}_{los}(t_0)\|_2$$

The angle of line-of-sight

$$\alpha(t_0) = \arccos\left(\frac{e_x \cdot r_{los}(t_0)}{|e_x| \cdot |r_{los}(t_0)|}\right)$$

The advance angle of U

$$\eta(t_0) = \alpha(t_0) - \sigma(t_0)$$

The magnitude of the normal correction acceleration

$$a(t_0) = \frac{v_u^2}{K(t_0)} = \frac{2 \cdot v_u^2 \cdot \sin\eta(t_0)}{r(t_0)}$$

(2) Iterative computation

In order to get a series of solutions for the control variable a using the iterative method, the differential equations in Eq. (1) and Eq. (3) should be discretized by using the following method

$$\dot{v}(t) = \frac{\partial v}{\partial t} = \frac{v(t+\Delta t) - v(t)}{\Delta t}$$

By this way, the guidance process can be divided into multiple discrete sub-processes as shown in Fig.6. Each sub-process is regarded as a straight line motion with time interval Δt.

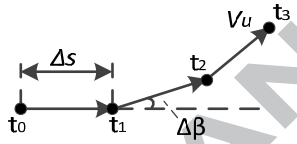

Fig. 6 The evolution of the UAV velocity

From the discrete sub-processes, the value at each instant can be calculated step by step. Let i (i=1, 2, 3…) represent the i-th iterative step; the iterative computation procedure can be illustrated as follows.

Step 1: Set i=1 and $\gamma = 0$;

Step 2: Calculate the position vector of U at t_i instant

$$p_u(t_i) = (x_{u_i}, y_{u_i}, z_{u_i})$$

where

$$\begin{aligned} x_{u_i} &= x_{u_{i-1}} + v_{ux_{i-1}} \cdot \Delta t \\ y_{u_i} &= y_{u_{i-1}} + v_{uy_{i-1}} \cdot \Delta t \\ z_{u_i} &= z_{u_{i-1}} + v_{uz_{i-1}} \cdot \Delta t \end{aligned}$$

Step 3: Calculate the position vector of P at t_i instant

$$p_p(t_i) = (x_{p_i}, y_{p_i}, z_{p_i})$$

where

$$\begin{aligned} x_{p_i} &= x_{p_{i-1}} + v_{px_{i-1}} \cdot \Delta t \\ y_{p_i} &= y_{p_{i-1}} + v_{py_{i-1}} \cdot \Delta t \\ z_{p_i} &= z_{p_{i-1}} + v_{pz_{i-1}} \cdot \Delta t \end{aligned}$$

Step 4: Update the velocity vector of P at t_i instant

$$v_p(t_i) = v_p(t_{i-1})$$

Step 5: Calculate the relative distance vector between U and P at t_i instant

$$r_{los}(t_i) = p_p(t_i) - p_u(t_i)$$

Step 6: Calculate the magnitude of the distance between U and P at t_i instant

$$r(t_i) = \|r_{los}(t_i)\|_2$$

Step 7: Calculate the angle of line-of-sight σ at t_i instant with Eq. (18)

$$\alpha(t_i) = \arccos\left(\frac{e_x \cdot r_{los}(t_i)}{|e_x| \cdot |r_{los}(t_i)|}\right)$$

Step 8: Update the guidance angle of U at t_i instant

$$\sigma(t_i) = \sigma(t_{i-1}) + \Delta\beta(t_{i-1})$$

Step 9: Calculate the velocity vector of U at t_i instant by Eq. (1)

$$\boldsymbol{v}_U(t_i) = (v_{Ux_i}, v_{Uy_i}, v_{Uz_i})$$

where

$$v_{Ux_i} = v_U \cdot \cos\sigma(t_i)$$
$$v_{Uy_i} = v_U \cdot \sin\sigma(t_i)$$
$$v_{Uz_i} = 0$$

Step 10: Calculate the advance angle of U at t_i instant

$$\eta(t_i) = q(t_i) - \sigma(t_i)$$

Step 11: Calculate the magnitude of the normal correction acceleration at t_i instant using Eq. (4)

$$a(t_i) = \frac{v_U^2}{R(t_i)} = \frac{2v_U^2 \cdot \sin\eta(t_i)}{r(t_i)}$$

Step 12: Calculated the corrected angle of the velocity vector for U at t_i instant

$$\Delta\beta(t_i) = \frac{a(t_i)}{v_U} \cdot \Delta t$$

Step 13: Calculated the angle between the velocity vectors of U and P at t_i instant

$$\nu(t_i) = \arccos\left(\frac{\boldsymbol{v}_U(t_i) \cdot \boldsymbol{v}_P(t_i)}{|\boldsymbol{v}_U(t_i)| \cdot |\boldsymbol{v}_P(t_i)|}\right)$$

Step 14: If $\nu(t_i)$ is smaller than a given value, 0.0005 rad in this paper, terminate the iterative computation and go into the guidance sub-phase; otherwise, let $i = i + 1$, and go to step 2.

3.1.2 Guidance sub-phase

At the end of the correction sub-phase, the position relationship between U and F as well as P in *Oc-RF* is shown in Fig.7.

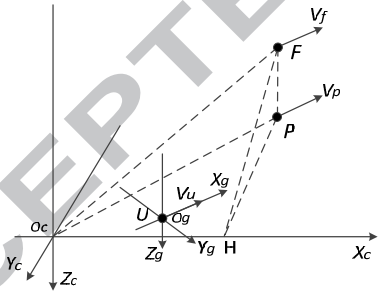

Fig.7 The position relationship after the correction sub-phase

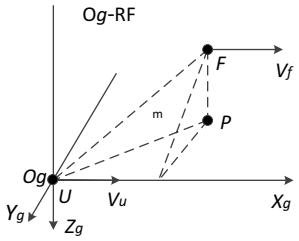

Fig.8 The new relationship in Og-RF

The state parameters at this moment can be denoted as follows:

The position vector of U

$$\boldsymbol{p}_{Uc} = (x_{Uc}, y_{Uc}, z_{Uc})$$

The velocity vector of U

$$\boldsymbol{v}_{Uc} = (v_{Ucx}, v_{Ucy}, v_{Ucz})$$

The position vector of P

$$\boldsymbol{p}_{Pc} = (x_{Pc}, y_{Pc}, z_{Pc})$$

The velocity vector of P

$$v_{pc} = (v_{pxc}, v_{pyc}, v_{pzc})$$

The position vector of *F*

$$p_{fc} = (x_{fc}, y_{fc}, z_{fc})$$

where $x_{fc} = x_{pc}, y_{fc} = y_{pc}, z_{fc} = z_f$, z_f are the required position components.
The velocity vector of *F*

$$v_{fc} = v_{pc}$$

In order to use the iterative computation algorithm similar to that used in the correction sub-phase, a coordinate system *Og-RF* is created with its origin at the current location of *U*. The orientation of the X-axis is consistent with the current velocity direction of *U*. The Z-axis is downward and perpendicular to the X-axis in the vertical plane. The Y-axis can be determined according to the right-hand rule as shown in Fig.7. The coordinate transformation from *Oc-RF* to *Og-RF* is obtained by

$$G = R_{gc} \cdot C + D \tag{5}$$

where C is a 3×1 column vector in *Oc-RF*, R_{gc} is the rotation matrix from *Oc-RF* to *Og-RF* which can be calculated as follows:

$$R_{gc} = \begin{bmatrix} \cos\sigma & \sin\sigma & 0 \\ -\sin\sigma & \cos\sigma & 0 \\ 0 & 0 & 1 \end{bmatrix} \tag{6}$$

and D is a 3×1 displacement vector:

$$D = -R_{gc} \cdot p_{uc} \tag{7}$$

Fig.8 indicates the new relationship between *U* and *F* in *Og-RF*. For the guidance sub-phase, the initial conditions for iterative computation at t_0 instant are computed as follows:
The position vector of *U*

$$p_{ug}(t_0) = R_{gc} \cdot p_{uc} + D$$

The velocity vector of *U*

$$v_{ug}(t_0) = R_{gc} \cdot v_{uc}$$

The position vector of *F*

$$p_{fg}(t_0) = R_{gc} \cdot p_{fc} + D = (x_{fg}, y_{fg}, z_{fg})$$

The velocity vector of *F*

$$v_{fg}(t_0) = R_{gc} \cdot v_{fc}$$

The angle between the guidance surface m and the OXY plane

$$\gamma = \arctan\frac{z_{fg}}{y_{fg}}$$

The iterative computation process is the same as that in the correction sub-phase.

3.2 Formation phase

The formation phase is to consider how to keep the UAV and the tanker flying in a formation for the preparation of the docking of the refueling probe of the UAV with the drogue of the tanker. When the distance between the UAV and the tanker is less than a specified value, a velocity coordinate system *Ov-RF* is created as shown in Fig.9. *Ov-RF* is used to measure the target location for computing the control variable. Fig.9 shows the position relation between *U* and *F* in *Ov-RF* during the formation phase. In order to guide the UAV to the formation point, the direction of the control acceleration a_f can be obtained according to the velocity coordinate system as shown in Fig.10. The magnitude of a_f is determined according to the coordinate value of *F* in *Ov-RF* as

$$a_f = A * \sin(\delta) \tag{8}$$

where *A* is a constant and δ is the angle between the UAV velocity and the X-axis of *Ov-RF*.

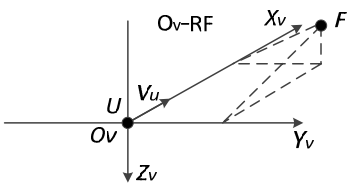

Fig.9 The UAV position relative to the formation point

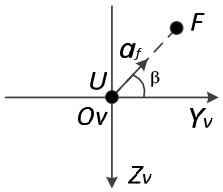

Fig.10 The direction of the control of the UAV

Besides, the formation flight phase in AAR requires the speed of the UAV be consistent with that of the tanker. For this reason, the control acceleration a_b along with the direction of the UAV speed should be utilized to control the speed of the UAV. The magnitude of a_b depends on the relative distance between *U* and *F* as well as their current speeds. In order to compute the exact value of a_b, the distance for *U* to move is given by

$$s = R \cdot 2 \cdot \arcsin\left(\frac{r}{2R}\right) + k \cdot r \tag{9}$$

where the term of "$k \cdot r$" represents an estimated distance, in which "k" is an estimation coefficient.

According to the Newton's theorem, the flying time for distance s can be calculated as

$$t = \frac{2s}{v_u + v_f}$$

The magnitude of the control acceleration a_b can be calculated by

$$a_b = \frac{v_f - v_u}{t} = \frac{v_f^2 - v_u^2}{2s} \tag{10}$$

In summary, the rendezvous process can be described by the flow chart shown in Fig.11.

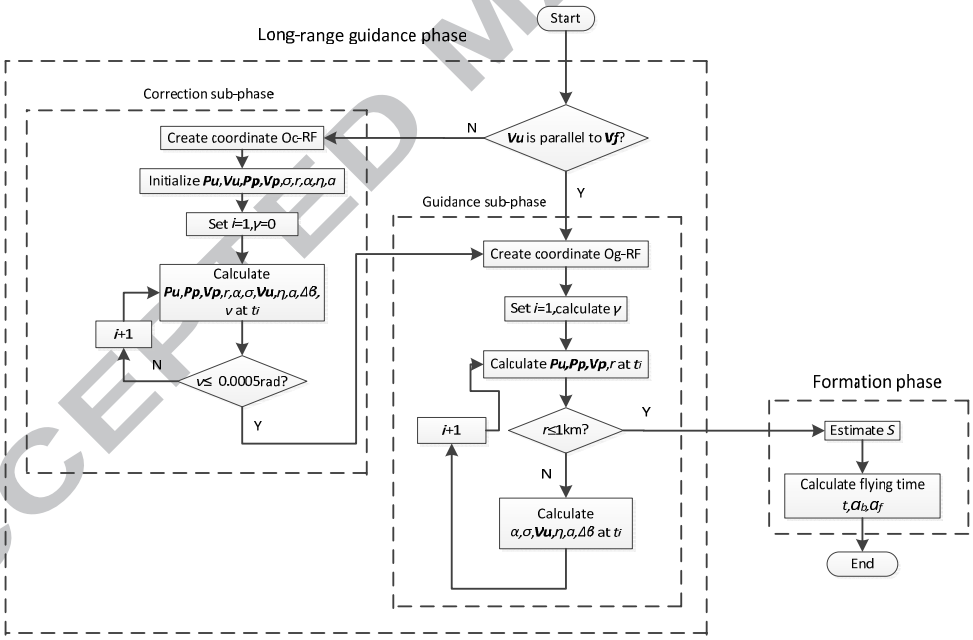

Fig.11 The flow chart for the ICGL approach

4. Simulations and analysis

In order to verify the effectiveness of the ICGL for the rendezvous and formation maintaining problem in AAR, a simulation is performed here using the proposed ICGL by comparing with the NG approach presented in Ref. [17] to demonstrate the effectiveness of the ICGL.

In this simulation, assume that the initial conditions of the UAV and the tanker are as follows:

Position vector of the UAV

$$p_M(t_0) = (x_{M_0}, y_{M_0}, z_{M_0}) = (0, 0, 0)$$

Velocity vector of the UAV

$v_M(t_0) = (v_{Mx_0}, v_{My_0}, v_{Mz_0}) = (100\text{m/s}, 0, 0)$

Position vector of the tanker

$p_T(t_0) = (x_{T_0}, y_{T_0}, z_{T_0})^T = (3000\text{m}, -8000\text{m}, -1000\text{m})$

Velocity vector of the tanker

$$v_T(t_0) = (v_{Tx_0}, v_{Ty_0}, v_{Tz_0})^T = (30\text{m/s}, -40\text{m/s}, 0)$$

During the formation phase, the relative position of the UAV to the tanker is set as

$d_x = 33\text{m}, d_y = 33\text{m}, d_z = 30\text{m}$

Simulations for the rendezvous and formation maintaining process of the UAV with the tanker are performed by using the ICGL and NG methods, respectively. Fig.12 shows the trajectories of the UAV approaching to the tanker in the rendezvous and formation maintaining process using the ICGL and the NG.

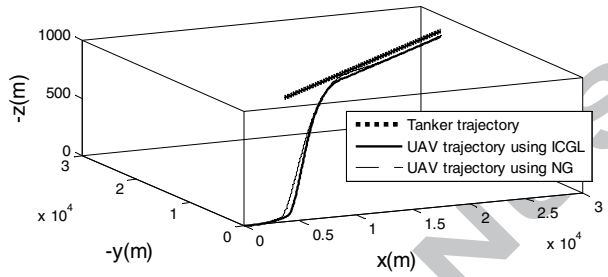

Fig.12 Trajectories through the rendezvous process using ICGL and NG

The control accelerations for the correction and guidance sub-phases are shown in Fig. 13 and Fig. 14, respectively. Using $E = \int_{t_0}^{t_f} a^2 dt$[18], we can compute the energy consumptions $E_{ICGL} = 1138.5$ for the ICGL and $E_{NG} = 1270$ for the NG, respectively. Obviously, the UAV consumes less energy to accomplish the rendezvous process by using the ICGL than by using the NG.

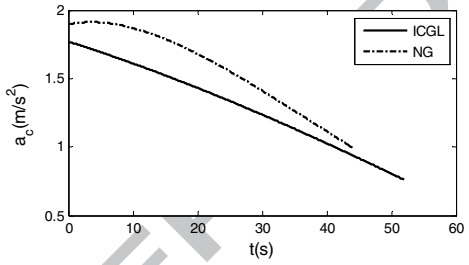

Fig.13 Control history in the correction sub-phase

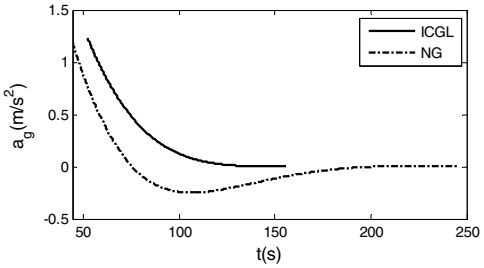

Fig.14 Control history in the guidance sub-phase

The altitude change histories of the UAV during the rendezvous process are shown in Fig.15 and Fig.16 for the ICGL and the NG. By comparison, it can be seen that, during the correction sub-phase, it takes 52 seconds for the UAV to complete its velocity direction adjustment using the ICGL and 34.5 seconds using the NG. For the guidance sub-phase, it takes 103.4 seconds to complete this process using the ICGL compared with 211.5 seconds using the NG. In general, it takes 217 seconds in total to accomplish the whole rendezvous process using the ICGL and 300 seconds using the NG. It is obvious that the proposed ICGL has better performance than the NG for the rendezvous problem.

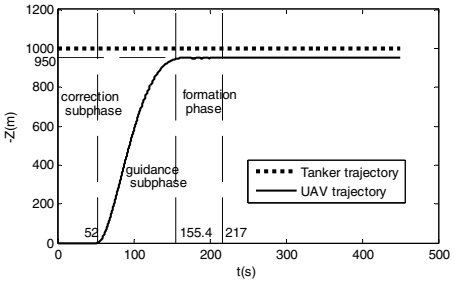

Fig.15 The UAV and tanker flight altitude change histories using the ICGL

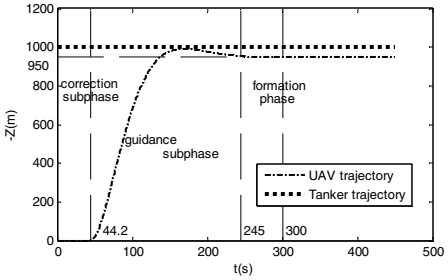

Fig.16 The UAV and tanker flight altitude change histories using the NG

Fig.17 and Fig.18 show the change histories of the distance and the angle between the UAV and the tanker during the whole rendezvous process using the ICGL, respectively. It can be seen from Fig.17 and Fig.18 that the UAV eventually keeps a formation flight with the tanker. This indicates the effectiveness of the proposed ICGL method.

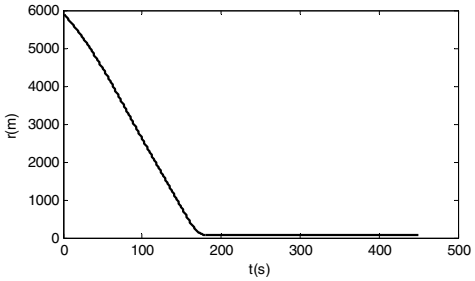

Fig.17 Distance between the UAV and the tanker

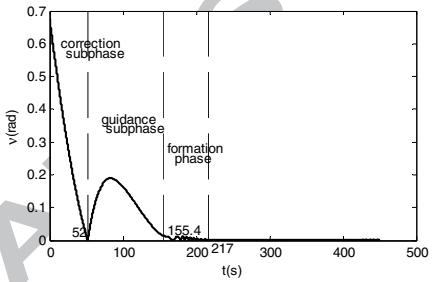

Fig.18 The change of angle for the velocity vectors

To test the robustness of the proposed ICGL to wind disturbance, we add a step wind disturbance along the X-axis with amplitude of $a_{wx} = 2\ m/s^2$ at the simulation time of 300s in the formation maintaining phase as shown in Fig.19. The simulation result for the whole rendezvous process is shown in Fig. 20. Fig.21 and Fig.22 show the deviations of the UAV to the desired distance with the tanker in the X and Y directions in the presence of wind disturbance. It can be seen that the steady state error is about 2m in the X direction and less than 3m in the Y direction. Fig.23 shows the change of the control acceleration of the UAV under wind disturbance. The simulation result indicates that the proposed ICGL has good robustness against wind disturbance.

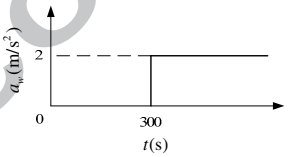

Fig.19 A step wind disturbance disturbance

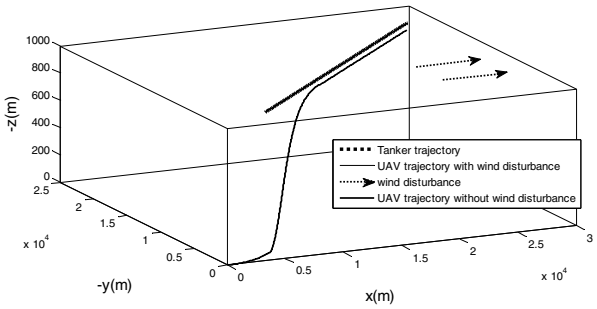

Fig.20 Trajectories of the rendezvous process against wind

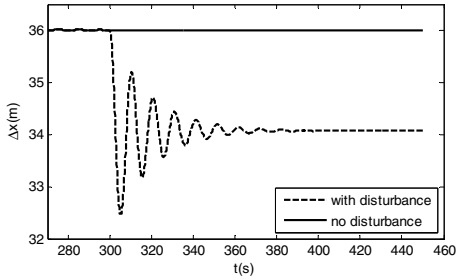

Fig.21 Distance between the UAV and the tanker on the X-axis

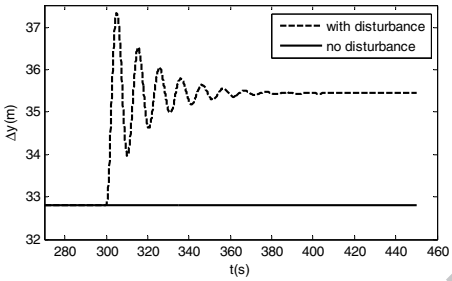

Fig.22 Distance between the UAV and the tanker on the Y-axis

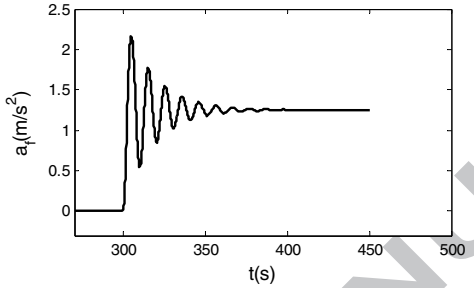

Fig.23 The control acceleration of the UAV under wind disturbance

5. Conclusions

(1) A guidance approach of the ICGL addressing the rendezvous and formation problem for a UAV in AAR is presented in this paper. The ICGL divides the whole process into two phases: the long-range guidance phase and the formation phase, in which the long-range guidance phase is further divided into two sub-phases: the correction sub-phase and the guidance sub-phase.

(2) The ICGL solves the guidance problem of each phase and sub-phase in a two-dimensional space with the iterative method to obtain the control acceleration for the UAV.

(3) Simulation results demonstrate that the proposed ICGL is effective for the UAV to deal with the rendezvous and formation problem in AAR and is robust against wind disturbance.

Acknowledgements

We would like to thank the anonymous reviewers for their constructive comments on this manuscript. This study was partially supported by the Natural Science Foundation of China (NSFC) under grant No: 61333004, partially by the Aeronautical Science Foundation of China under grant No: 20115868009, and partially by the open funding project of the State Key Laboratory of Virtual Reality Technology of and Systems at Beihang University, under grant No: BUAA-VR-13KF-01.

References

[1] Luo D L, Lu TX, Wu S X. A survey on guidance laws for flight vehicle. Journal of System Simulation 2010; S1: 16-20 [Chinese].

[2] Guelman M. A qualitative study of proportional navigation. IEEE Transactions on Aerospace and Electronic Systems1971; AES-7(4): 337-343.

[3] TyanF. Capture region of a GIPN guidance law for missile and target with bounded maneuverability. IEEE Transactions on Aerospace and Electronic Systems 2011;47(1): 201-213.

[4] Lin CL, Li YH. Development of 3-D modified proportional navigation guidance law against high-speed targets. IEEE Transactions on Aerospace and Electronic Systems2013; 49 (1): 677-687.

[5] Zhao S Y, Zhou R, Wei C, Ding Q X. Design of time-constrained Guidance Laws via virtual leader approach. Chinese Journal of Astronautics 2010; 23(1): 103-108.

[6] Yamasaki T, Balakrishnan SN, Takano H. Integrated guidance and autopilot design for a chasing

UAV via high-order sliding modes. Journal of the Franklin Institute 2012; 349 (2):531-558.

[7] Jing W X, Li C Y, Qi Z G. Application of the 3D Differential Geometric Guidance Commands. Journal of Astronautics 2007; 28(5): 1235-1240 [Chinese].

[8] Li X S, Li X. Robust adaptive back stepping design for unmanned aerial vehicle formation guidance and control. Journal of Applied Sciences 2012; 30(5): 552-558 [Chinese].

[9] Hassan G M, Yahya K M, Haq I U. Leader-follower approach using full-state linearization via dynamic feedback. Proceedings of the International Conference on Emerging Technologies 2006; 297-305.

[10] Linorman N H M, Liu, HH T. Formation UAV flight control using virtual structure and motion synchronization. Proceedings of the American Control Conference 2008, 1782-1787.

[11] Karimoddini A, Lin H, Chen B M, Lee T H. Hybrid three-dimensional formation control for unmanned helicopters. Automatica 2013; 49(2): 424-433.

[12] Han Z Z. An Iterative guidance method for the large launch vehicle. Journal of Astronautics 1983; 1: 9-21 [Chinese].

[13] Fu Y, Chen G, Lu B G, Guo J F, et al. A vacuum adaptive iterative guidance method of launch vehicle based on optimal analytical solution. Acta Aeronautica Et Astronautica Sinica2011; 32(9): 1696-1704 [Chinese].

[14] Song Z Y. From accurate, precise to perfect-manned space promotes the development of guidance method on launch vehicle. Aerospace Control 2013. 31(1): 4-10 [Chinese].

[15] Xiao L X, Wang J P, Wang A M, et al. Optimal iterative guidance method based on required trajectory. Aerospace Shanghai 2012; 29(3): 1-5 [Chinese].

[16] Chandler DC, Smith I E. Development of the iterative guidance mode with its application to various vehicles and missions. Journal of Spacecraft and Rockets 1967.4(7): 898-903.

[17] Park S, Deysty J, How J P. A new nonlinear guidance logic for trajectory tracking. Proceedings of the AIAA Guidance, Navigation, and Control Conference and Exhibit 2004; AIAA-2004-4900.

[18] Luo D L, Li Y F, Wu W H, et al. Terminal guidance law based on receding horizon control for homing missile. Journal of Nanjing University of Aeronautics and Astronautics 2005; 37(1): 52-56 [Chinese].